

Image Sensor Noise model for Image System Simulation

Norman L. Koren, Imatest LLC, Boulder, Colorado, USA

Abstract

We present an image sensor noise model that can be used in a complete image system simulation that includes image generation, lens degradations, and ISP (Image Signal Processing), and can produce classic measurements (SFR, noise, etc.) as well as new information metrics such as information capacity and SNRi. [1]

The noise model is derived from a classic Photon Transfer Curve (PTC) [2] obtained from one or more raw (undemosaiced) images of a high dynamic range grayscale test chart. Image sensor noise is composed of three factors.

1. Dark noise, which includes electronic noise, dark current noise, DSNU fixed-pattern noise, and noise from several other sources. It is independent of signal amplitude, A .
2. Photon shot noise, which varies with \sqrt{A} , and
3. PRNU fixed-pattern noise, which varies linearly with A .

The coefficients for the three factors are determined using a Levenberg Marquardt optimizer [3] that provides an extremely close fit between the measured data and the calculated PTC. The coefficients can also be derived from EMVA 1288 measurements, which are more accurate and detailed, but require the acquisition of a large number of images.

We show how the model can predict performance over a wide range of conditions, and most importantly, for low light.

Introduction

The image sensor noise model, to be described, is intended for use in a camera simulation such as Imatest's *Simatest* [1], which can be summarized by the following block diagram.

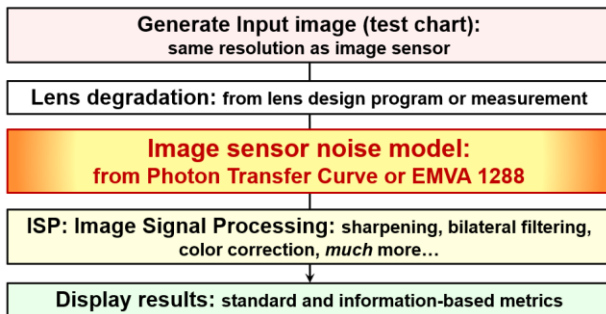


Figure 1. Camera simulation block diagram

Prior to running the simulation, the noise model must be calculated in a separate program by analyzing a totally raw (undemosaiced) image of a High Dynamic Range (HDR) test chart. It can also be derived from EMVA 1288 measurements [4].

The input image to the camera simulation may be

- An acquired image — either raw or demosaiced, usually with minimal processing. Since acquired images contain noise, the noise model is not applied by the simulator.
- A simulated image, preferably including a test chart with 4:1 contrast slanted edges, which can be used for calculating camera performance.

Although any image can be used for the simulation input, images of test charts that contain 4:1 contrast slanted edges are recommended for calculating camera performance. Images of High Dynamic Range (HDR) test charts are also of interest.

Sequence of operations — For simulated images, a lens degradation must be applied. This can be accomplished by processing the image with a lens design utility such as CODE V [5] or Zemax Optic Studio [6], or by measuring a minimally-processed demosaiced image and applying a gaussian blur in the simulator so its output matches the measured sharpness, expressed as Spatial Frequency Response (SFR), which is often used interchangeably with Modulation Transfer Function (MTF). [ISO standards have been moving from MTF to SFR, but MTF is still more familiar.]

For simulated images, the image sensor noise model is applied.

For all images, Image Signal Processing (ISP) can be applied.

Results — The resulting image can be analyzed for standard metrics such as SFR (MTF) as well as new information-based metrics.

We will compare measurements of acquired and simulated slanted-edge test patterns at EI 100 (the baseline sensitivity) and EI 3200 (a very high exposure index, which represents extremely low light).

The image sensor noise model

Raw (undemosaiced and unprocessed) images have a remarkable property: the noise, N_i in each patch is a function of the mean digital number (DN_i) or normalized signal amplitude, $V_i = DN_i/DN_{max}$ (where DN_{max} is the maximum DN for the system, typically 2^{n-1} for bit depth = n), independent of the color.

This allows a Photon transfer Curve (PTC) [2] — a plot of calculated noise, σ_{PTC} , as a function of exposure (-chart density) — to be calculated from a raw image of a High Dynamic Range (HDR) test chart, such as a 36-patch Dynamic Range chart (Figure (2)) or the new Information-based Dynamic Range (InfoDR) chart [17]

(Figure (3)). The HDR chart should have an optical density range of at least 3, and preferably 4 (greater than reflective charts can support) so low pixel levels, representing dark noise, are present.

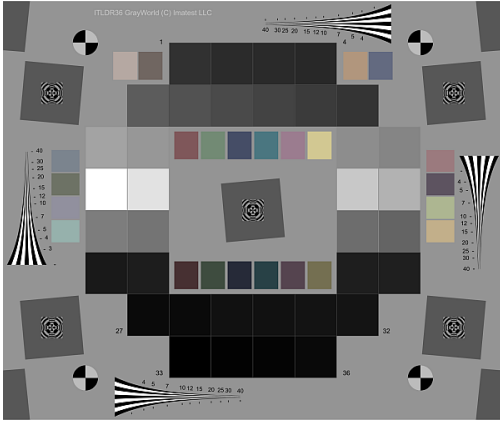


Figure 2. 36-patch High Dynamic Range chart (new V2 patch arrangement, modified to minimize ghost images from lightest to darkest patches.)

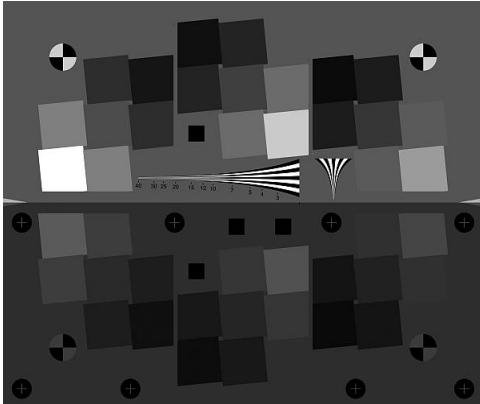


Figure 3. Information-based Dynamic Range (InfoDR) chart [17]

The PTC (Figure 4), which displays noise, σ_{PTC} , as a function of exposure, V (chart density), is the heart of the image sensor noise model, enabling camera performance to be predicted for a wide range of conditions.

$$\sigma_{PTC}(V) = \sqrt{k_{Ndark}^2 + k_{Nshot}^2 V + k_{PRNU}^2 V^2} \quad (1)$$

where

- k_{Ndark} is the coefficient of total dark noise, which is fixed — independent of exposure V . It combines electronic (Johnson) noise, which is temperature-dependent, dark current noise (affected by exposure time for relatively long exposures), Dark Signal Nonuniformity (DSNU, a form of fixed-pattern noise), and several additional noise sources,

- k_{Nshot} is the coefficient of photon shot noise, which increases with \sqrt{V} .
- k_{PRNU} is the coefficient of Photo Response Nonuniformity (PRNU) — a fixed-pattern noise, which increases with V .

Figure 4 shows a PTC for an image acquired from the 24-megapixel APS-C camera with an excellent 60mm f/2.8 macro lens set to f/8, converted from raw to RGB with LibRaw [7], *without* demosaicing or any other processing, that is used in the examples below.

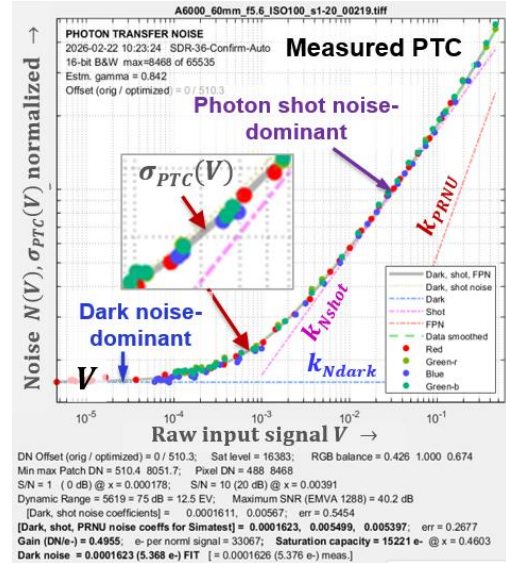


Figure 4. Photon Transfer Curve from acquired raw image ($\sigma_{PTC}(V)$): Gray curve, frequently obscured by N_R , N_{Gr} , N_B , and N_{Gb} noise data.

Measuring the noise model parameters

Photograph an HDR test chart (Figure 2 or 3) in a darkened room: every effort should be made to minimize stray light. For cameras with moderate to high resolution, the active chart image should be in the center of the frame, i.e., it should generally *not* fill the frame.

Acquire the image in a raw format (usually Bayer raw, but other CFAs work equally well),

Many “raw” files from commercial cameras contain a digital offset, $V_{off} = DN_{off} / DN_{max}$, whose value is typically unknown. V_{off} must be subtracted from the normalized input amplitude, V_{input} , to obtain a correct PTC.

$$V = V_{input} - V_{off} \quad (2)$$

The Appendix shows how subtracting an estimate of V_{off} affects the PTC, and it contains an algorithm for estimating a value of V_{off} that results in a reliable, consistent PTC and noise coefficients.

The three noise coefficients in Equation (1) can be calculated by means of a Levenberg-Marquardt optimizer [3,8-10], which is a well-known algorithm for finding

a least-squares solution of an overdetermined system of nonlinear equations. The optimizer is set up to minimize

$$Error = \sum_{i=1}^{Ndata} (N_i^2(V_i) - \sigma_{PTC}^2(V_i)) / N_i^2(V_i) \quad (3)$$

The division by the measured noise power, $N_i^2(V)$, is required to give dark and light regions similar weighting so that k_{Ndark} can be accurately calculated along with k_{Nshot} and k_{PRNU} .

The speed and final results are somewhat (but not strongly) dependent on the initial estimates of the coefficients. Assuming that the $Ndata$ values of V_i and N_i have been sorted in order of increasing V , we obtained good results using initial values,

$$k_{Ndark}(init) = \min(N_i) \quad (4)$$

$$k_{Nshot}(init) = \sqrt{\frac{N_{Ndata}^2 - N_{Ndata/2}^2}{V_{Ndata} - V_{Ndata/2}}} \quad (5)$$

$$k_{PRNU}(init) = \frac{k_{Nshot}(init)}{2} \quad (6)$$

Levenberg-Marquardt optimizers can be found in the MATLAB Optimization Toolbox [8] as well at the MATLAB File Exchange [9,10], and should be available for any widely-used programming language.

Noise parameters from EMVA 1288

The European Machine Vision Association EMVA 1288 standard (now also ISO 24942) [4], is a comprehensive and well-established set of measurements for characterizing the signal and noise response of image sensors. It is especially good for separating fixed-pattern from temporal noise sources. But it requires the acquisition of a large number of flat-field images at well-controlled illumination levels.

EMVA 1288 measurements can be converted into input for Imatest's Simatest simulator, allowing them to be used for predicting system performance. The table below presents the key measurements and units.

Measurement	EMVA symbol	Units
Temporal dark noise	σ_d OR σ_{Dark}	e-
Dark Signal Nonuniformity DSNU	$DSNU_{ISO}$	e-
Dark current (noise)	μ_c OR i_{Dark}	e-/s
Gain (DN/e-)	K	DN/e-
(Photon shot noise = $\sqrt{K/DN_{max}}$)		

Photo Response Nonuniformity PRNU	$PRNU_{ISO}$	%
Saturation capacity	$\mu_{e.sat}$	e-
From ISO 24942, section 15.2 and Annex A or EMVA 12288 4.0, section G.		

DN = Digital Number
$e-$ = electrons
s = exposure time in seconds
V = normalized amplitude = DN/DN_{max} , where DN_{max} is the maximum digital number for the system, typically 2^{n-1} for bit depth = n ,

The key EMVA 1288-derived measurements for the simulator input are

$$k_{NDark} = \sqrt{\sigma_d^2 + DSNU^2 + (i_{Dark} s)^2} \times Gain \left(\frac{V}{e-} \right) \quad (7)$$

$$k_{Nshot} = \sqrt{\frac{Gain(DN/e-)}{DN_{max}}} = \sqrt{\frac{K}{DN_{max}}} \quad (8)$$

$$k_{PRNU} = \frac{PRNU(\%)}{100} \quad (9)$$

Information theory and metrics

Since we have discussed information theory and metrics in several papers [13,14,17], we will present only the briefest summary here. Information theory was developed by Claude Shannon in 1948-49 [11,12]. It has long been of interest in imaging [15,16], but it never got much traction because measurements were cumbersome and error-prone.

That changed in 2023, when Imatest developed a trick for measuring the signal and noise from the same location in slanted edges. In essence, an image is a communication channel with an information capacity. C , in units of bits per pixel.

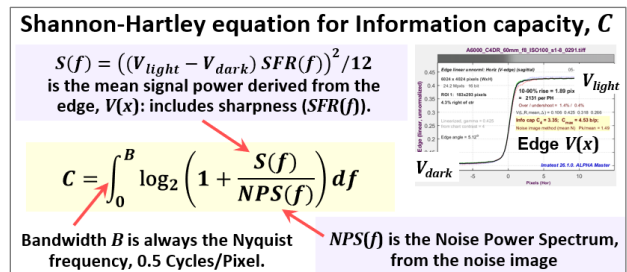


Figure 5. Shannon-Hartley equation for information capacity, C .

The accompanying Electronic Imaging 2026 paper, "Information-based Dynamic Range" [17], describes C_4 , which is the information capacity directly measured from an ISO 12233-standard [18] 4:1 contrast slanted edge. C_4 is the amount of information that can be con-

veyed in a pixel for a 4:1 contrast object, making it an excellent metric for quantifying exposure-dependent camera performance.

Note that since C is a function of image contrast ($V_{light} - V_{dark}$), sharpness ($SFR(f)$), and Noise Power Spectrum ($NPS(f)$) (Figure 5), we regard it as a *complete* image quality metric (at the pixel level), in distinction to the three factors in its calculation, which we regard as *partial* metrics.

Simulated images and Photon Transfer Curve

A bitmap version of the original test chart image was read into the Simatest simulator [1], then converted to a pseudo-Bayer raw image by placing the appropriate RGB channel data into each pixel using a Bayer color filter array (CFA) pattern: {RGRG; GBGB; ...}.

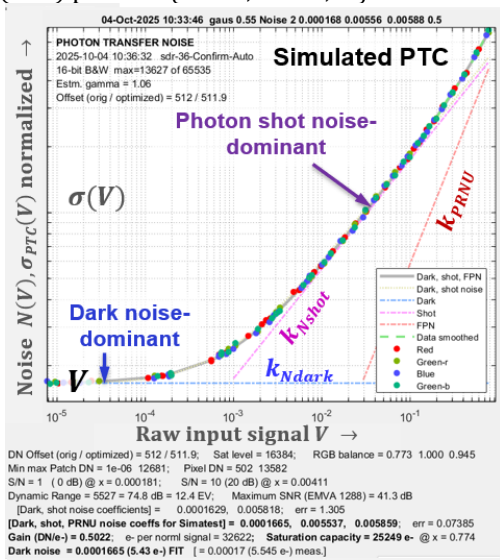


Figure 6. Photon Transfer Curve ($\sigma_{PTC}(V)$) showing data, $N(V)$, from simulated pseudo-raw image. Nearly identical to the acquired image in Figure 4.

The values for the three noise coefficients, taken from Figure 4, were applied to a simulated pseudo-raw image, which was analyzed to produce the Photon Transfer Curve shown in Figure 6. As shown in the table below, the noise coefficients are nearly identical to the acquired image in Figure 4.

Coefficients	k^2_{Ndark}	k^2_{Nshot}	k^2_{PRNU}
Acquired, Fig. 4	0.0001623	0.005499	0.005397
Simulated, Fig. 6	0.0001665	0.005537	0.005859

Simulated vs. acquired image performance

Figure 7 contains the mean edge response and MTF (SFR) for a 4:1 contrast slanted edge for acquired and simulated images.

- Left: captured from the same 24-megapixel camera referenced above, and converted into 48-bit Adobe

RGB with LibRaw [7] with minimal processing (demaosaiced, but no sharpening or noise reduction).

- Right: Simulated, with a gaussian filter with $\sigma = 0.55$ pixels applied so the MTF matches the acquired image. The relative amplitudes of the R, G, and B channels were also applied.

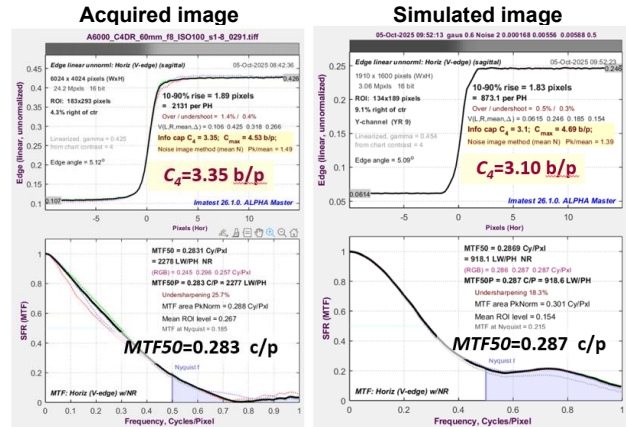


Figure 7. Average Edge and MTF for acquired image (left) and simulated image (right)

The results are similar, with both $MTF50$ and C_4 nearly identical. But MTF above the Nyquist frequency ($f_{Nyq} = 0.5$ c/p) is different for the two plots, possibly as a result of different edge shape assumptions or demosaicing algorithms. But it doesn't make much difference for performance because the calculation of information capacity, C , omits $f > f_{Nyq}$ (B in Fig. 5).

Low-light performance

The four MTF results in Figure 8 consist of acquired and simulated images at Exposure Index (EI) 100 and 3200.

(UL) Acquired EI 100 image is the baseline for comparison. It has been demosaiced and minimally processed (no sharpening or noise reduction).

(UR) Simulated EI 100 image started as an ideal image. A gaussian blur ($\sigma = 0.55$ pixels) to match $MTF50$, the PTC noise parameters, and RGB balance (Figure 4) were applied.

(LL) Acquired EI 3200 image, demosaiced and minimally processed.

(LR) Simulated EI 3200 image: Image amplitude was reduced by $1/32x$, gaussian blur, PTC noise, and RGB balance were added, then amplitude was increased $32x$ to simulate EI 3200.

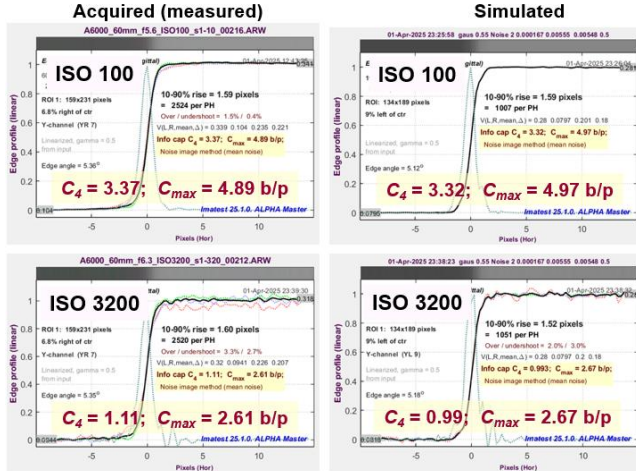


Figure 8. Acquired vs. simulated performance at ISO 100 (normal, bright light) and 3200 (dim light).

As expected, C_4 information capacity is similar for both EI 100 images. The real test was the performance at EI 3200 (simulating very dim light), where C_4 was much lower for both images. The difference between them was only about 12%.

Summary

We have shown how to calculate a Photon Transfer Curve (PTC) from a raw image of a High Dynamic Range test chart, using a Levenberg-Marquardt optimizer. The PTC, which displays noise as a function of input amplitude for a raw image, represents the image sensor noise model, which can be entered into a camera simulator that predicts performance based on standard or information metrics such as NEQ or SNR_i [21-24], and most notably, the information capacity for 4:1 contrast objects, C_4 , for a wide range of lighting, including extremely low light [17].

Future work

- Simulate High Dynamic Range sensors, which have response similar to standard linear sensors, but have more than one operating region, separated by steps where the noise jumps and the SNR drops abruptly. Figure 9 is an example based on work done for the IEEE P2020 standards committee [19,20].
- Calculate an approximate Detective Quantum Efficiency (output electrons per photon incident on the sensor), and use it to determine the limits of low light performance for simulated cameras, which is of particular interest to the automotive industry.

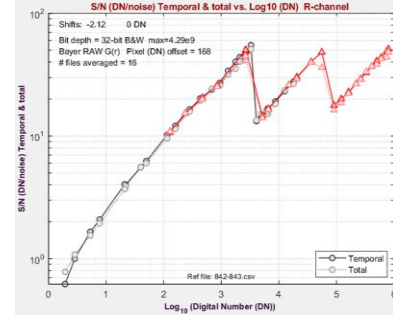


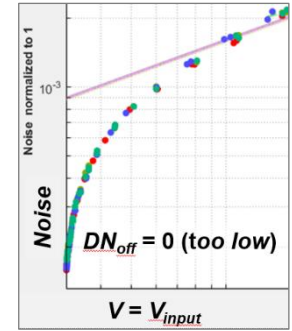
Figure 9. SNR (Signal-to-Noise Ratio) response of HDR sensor

Appendix. Digital Offset, V_{off} or DN_{off}

When a digital offset is present, the PTC is calculated from $V = V_{input} - V_{offEst}$, where $V_{input} = DN_{input} / DN_{max}$ is the normalized mean raw input amplitude of each patch, with minimum and maximum values, V_{min} and V_{max} .

Let V_{offEst} be the estimated digital offset.

Figure 10. PTC with bad V_{offEst} estimate



- If V_{offEst} is too low or not subtracted from V_{input} (right), the dark noise-dominant region (on the x-axis) will be severely compressed, and the dark noise coefficient, k_{Ndark} , cannot be calculated.
- If V_{offEst} is too high, i.e., if $V_{offEst} > V_{min}$, some values of V will be < 0 , causing them to be removed from the calculation, degrading the accuracy of k_{Ndark} .

Since V_{off} is often unavailable, and finding it by trial-and-error is tedious, we have developed an algorithm for reliably calculating it.

Algorithm for finding V_{off}

Let D_{chart} be the set of measured patch densities of the test chart (usually supplied in a file for individual film or photomask charts). The minimum and maximum density values are D_{min} and D_{max} , and the density range is $D_{range} = D_{max} - D_{min}$. The Luminance ratio is $L_{ratio} = 10^{D_{range}} = 10^{(D_{max} - D_{min})} = 10^{D_{max}} / 10^{D_{min}}$.

Let the mean input amplitude for each patch be V_{input} , with minimum and maximum values, V_{min} and V_{max} .

Reliable, consistent PTCs can be obtained using the value of V_{off} that makes the x-axis signal ratio identical to the luminance ratio (where we use $\min(L_{ratio}, 10^5)$ to keep the results reasonable).

$$\begin{aligned} & (V_{max} - V_{off}) / (V_{min} - V_{off}) \\ & = \min(L_{ratio}, 10^5) = L_{rTarget} \end{aligned} \quad (A-1)$$

Solving for V_{off} ,

$$V_{off} = (V_{max} - V_{min} L_{rTarget}) / (1 - L_{rTarget}) \quad (A-2)$$

For $V = V_{input} - V_{off} = (DN_{input} - DN_{off}) / DN_{max}$, Equation (A-2) gives a reliable estimate of k_{Ndark} , k_{Nshot} , and k_{PRNU} , with a Photon Transfer Curve that resembles Figure 4, even though the x-axis (normalized amplitude V) may not be strictly accurate in the dark region.

References

- [1] Simatest Overview, <https://www.imatest.com/imaging/simatest-overview/>
- [2] J. R. Janesick, Photon Transfer $DN \rightarrow \lambda$, SPIE Digital Library, 2007. <https://doi.org/10.1117/3.725073>
- [3] Levenberg-Marquardt algorithm, https://en.wikipedia.org/wiki/Levenberg%E2%80%93Marquardt_algorithm
- [4] European Machine Vision Association, EMVA 1288 Standard for Measurement and Presentation of Specifications for Machine Vision Sensors and Cameras, <https://www.emva.org/standards-technology/emva-1288/>
- [5] Using Imatest with Keysight's CODE V 2D Image Simulation (IMS), <https://imatest.atlassian.net/wiki/spaces/KB/pages/11846123551/>
- [6] Zemax Optic Studio, <https://optics.ansys.com/hc/en-us/articles/42661994652819-How-to-simulate-high-resolution-images>
- [7] LibRaw – raw image decoder, <https://www.libraw.org/>
- [8] MATLAB Optimization Toolbox, <https://www.mathworks.com/help/optim/ug/least-squares-model-fitting-algorithms.html>
- [9] MATLAB File Exchange: Levenberg-Marquardt toolbox, <https://www.mathworks.com/matlabcentral/fileexchange/53449-levenberg-marquardt-toolbox>
- [10] MATLAB File Exchange: LMFSolve.m, <https://www.mathworks.com/matlabcentral/fileexchange/16063-lmfsolve-m-levenberg-marquardt-fletcher-algorithm-for-nonlinear-least-squares-problems>
- [11] C. E. Shannon, "A mathematical theory of communication," Bell Syst. Tech. J., vol. 27, pp. 379–423, July 1948; vol. 27, pp. 623–656, Oct. 1948.
- [12] C. E. Shannon, "Communication in the Presence of Noise," Proceedings of the I.R.E., January 1949, pp. 10-21.
- [13] N. L. Koren, "Measuring camera information capacity with slanted-edges (Invited)" *Electronic Imaging*, 2023, pp 454--1 - 454-9, <https://doi.org/10.2352/EI.2023.35.8.IQSP-454>
- [14] N. L. Koren, "Image Information Metrics From Slanted Edges: A Toolkit of Metrics to Aid Object Recognition, Machine Vision, and Artificial Intelligence Systems" *Electronic Imaging*, 2024, <https://doi.org/10.2352/EI.2024.36.9.IQSP-256>. We recommend the revised and corrected version of this paper: https://www.imatest.com/wp-content/uploads/2024/03/Koren_Image_Information_Metrics_paper_final.pdf
- [15] J. C. Dainty and R. Shaw, "Image Science," Academic Press, 1974.
- [16] Francis T. S. Yu, "Optics and Information Theory," Wiley, 1976.
- [17] N. L. Koren, "Information-based Dynamic Range: Measuring camera performance over a wide range of illumination from a single image", presented at *Electronic Imaging*, 2026.
- [18] ISO/DIS 12233 Digital Cameras Resolution and spatial frequency responses, <https://www.iso.org/standard/88626.html>.
- [19] Orit Skorka, Paul Romanczyk, "A review of IEEE P2020 noise metrics" *Proc. IS&T Int'l. Symp. on Electronic Imaging*, 2022, <https://doi.org/10.2352/EI.2022.34.16.AVM-109>
- [20] Orit Skorka, Paul Romanczyk, et al, "Evaluation of Signal and Noise Metrics of High Dynamic Range Image Sensors by IEEE P2020 Methodology" *Electronic Imaging*, 2024, <https://doi.org/10.2352/EI.2024.36.17.AVM-107>
- [21] Robin Jenkin, Paul Kane, "Fundamental Imaging System Analysis for Autonomous Vehicles," *Proc. IS&T Int'l. Symp. on Electronic Imaging: Autonomous Vehicles and Machines*, 2018, <https://doi.org/10.2352/ISSN.2470-1173.2018.17.AVM-105>
- [22] Brian W. Keelan, "Imaging Applications of Noise Equivalent Quanta," *Proc. IS&T Int'l. Symp. on Electronic Imaging: Image Quality and System Performance XIII*, 2016, <https://doi.org/10.2352/ISSN.2470-1173.2016.13.IQSP-213>.
- [23] Orit Skorka, Paul J. Kane, "Object Detection Using an Ideal Observer Model", *Proc. IS&T Int'l. Symp. on Electronic Imaging: Autonomous Vehicles and Machines*, 2020, pp 41-1 - 41-7, <https://doi.org/10.2352/ISSN.2470-1173.2020.16.AVM-041>
- [24] Paul J. Kane, "Signal detection theory and automotive imaging", *Proc. IS&T Int'l. Symp. on Electronic Imaging: Autonomous Vehicles and Machines Conference*, 2019, pp 27-1 - 27-8, <https://doi.org/10.2352/ISSN.2470-1173.2019.15.AVM-027>

Author Biography

Norman Koren became interested in photography while growing up near the George Eastman Museum in Rochester, NY. He received his BA in physics from Brown University (1965) and his Masters in physics from Wayne State University (1969), then worked in the computer storage industry simulating digital magnetic recording systems and channels, until 2001. He founded Imatest LLC in 2003 to develop software, test charts, and lab hardware for measuring the quality of digital imaging systems. Since 2021 he has been obsessed with applying information theory to image quality measurement.

JOIN US AT THE NEXT EI!

electronic IMAGING

Imaging across applications . . . Where industry and academia meet!



- **SHORT COURSES • EXHIBITS • DEMONSTRATION SESSION • PLENARY TALKS •**
- **INTERACTIVE PAPER SESSION • SPECIAL EVENTS • TECHNICAL SESSIONS •**

www.electronicimaging.org

